Regular Article – Theoretical Physics

Calculation of relativistic nucleon-nucleon potentials in three dimensions

M.R. Hadizadeh[1,2,a] and M. Radin[3,b]

[1] Institute of Nuclear and Particle Physics and Department of Physics and Astronomy, Ohio University, Athens, OH 45701, USA
[2] College of Science and Engineering, Central State University, Wilberforce, OH 45384, USA
[3] Department of Physics, K. N. Toosi University of Technology, P.O.Box 16315–1618, Tehran, Iran

Abstract. In this paper, we have applied a three-dimensional approach for the calculation of the relativistic nucleon-nucleon potential. The quadratic operator relation between the non-relativistic and the relativistic nucleon-nucleon interactions is formulated as a function of relative two-nucleon momentum vectors, which leads to a three-dimensional integral equation. The integral equation is solved by the iteration method, and the matrix elements of the relativistic potential are calculated from non-relativistic ones. The spin-independent Malfliet-Tjon potential is employed in the numerical calculations, and the numerical tests indicate that the two-nucleon observables calculated by the relativistic potential are preserved with high accuracy.

1 Introduction

The inputs for the relativistic three-body (3B) bound and scattering state calculations [1–9] are the fully off-shell relativistic nucleon-nucleon (NN) t-matrices, which can be obtained by solving the relativistic Lippmann-Schwinger (LS) integral equation using relativistic NN interactions.

It is known that there is a nonlinear operator relation between the non-relativistic and the relativistic NN interactions. So, the first step toward the calculation of relativistic t-matrices is the calculation of the relativistic potentials from non-relativistic ones. To this aim, the matrix elements of the relativistic NN potential in momentum space are traditionally calculated by solving the nonlinear equation using the following different methods.

In the spectral expansion method, the quadratic equation is solved by inserting a completeness relation of the NN bound and scattering states into the right side of the quadratic equation and by projecting the result into the momentum space [10, 11]. So, by having the non-relativistic potential one can first calculate the NN bound state wave function and scattering half-shell t-matrix and use the result to solve the nonlinear equation.

In the iteration method, the nonlinear equation is solved by iteration. Kamada and Glöckle introduced a powerful numerical technique to calculate the matrix elements of the relativistic NN potential directly from the

matrix elements of the non-relativistic NN potential [12]. In this method, the nonlinear integral equation is solved using the iteration method to get relativistic and boosted potentials from non-relativistic ones. It is successfully implemented in the NN problem, but it has not yet been extended to a three-dimensional (3D) approach.

Another method is to multiply the non-relativistic potential by a function that depends on NN relative momenta, in such a way that both the non-relativistic and the relativistic potentials lead to same phase shifts and observables [13]. The function is defined in such a way that it changes the non-relativistic kinetic energy to the relativistic kinetic energy by rescaling the momentum variables, which leads to the same $2N$ binding energy for both non-relativistic and relativistic potentials.

In the past decade a 3D approach based on momentum vector variables was developed to study the few-body bound and scattering problems [7, 14–39]. In the 3D approach one works directly with vector variables which lead to 3D integral equations, whereas the partial wave (PW) representation in the angular momentum basis leads to coupled equations. In the PW representation, depending on the energy scale of the problem, one must sum PWs, and consequently at higher energies one needs to consider a larger number of PWs, however the 3D approach automatically contains all PWs and the number of equations is energy independent.

We would like to point out that as Polyzou and Elster have shown one can directly calculate the relativistic

[a] e-mail: `hadizadm@ohio.edu`
[b] e-mail: `radin@kntu.ac.ir`

t-matrix from the non-relativistic one, without needing to solve the nonlinear equation. Consequently, one does not need to solve the LS equation for the embedded NN interaction, and one can calculate the fully off-shell relativistic t-matrix by following a two-step process. The first step is to obtain the relativistic right-half-shell (RHS) t-matrix from the non-relativistic RHS t-matrix by an analytical relation proposed by Coester *et al.* [40]. The second step is to calculate the fully-off-shell t-matrix from the RHS t-matrix by solving a first resolvent equation. Keister *et al.* [41] proposed the method and it is implemented for the first time in a 3B scattering calculation [7] in this way. Using the direct calculation of the relativistic t-matrix from the non-relativistic one, recently the relativistic effects were studied in the 3B binding energy using a 3D scheme [14,16]. The relativistic 3B wave function was calculated for the first time, and it was shown that the relativistic effects lead to a reduction of about 3% in the 3B binding energy for two models of a spin-independent Malfliet-Tjon–type potential. Since the 3D approach automatically considers all PWs, if it works for the bound state, it can also be extended to the scattering problem, independent of the range of energy. The next step is to consider the spin and isospin degrees of freedom and work with realistic NN interactions.

In this work, we have applied the iteration method proposed by Kamada and Glöckle to construct the relativistic NN potential from the non-relativistic Malfliet-Tjon potential in a 3D scheme, without using the PW decomposition.

2 Three-dimensional formulation of the quadratic operator relation between the relativistic and non-relativistic NN potentials

According to Bakamjian and Thomas [42] and Fong and Sucher [43], the relativistic NN dynamics is specified in terms of the NN mass operator h

$$\langle \mathbf{p}|h|\mathbf{p}'\rangle = \omega(\mathbf{p})\,\delta(\mathbf{p}-\mathbf{p}') + V_r(\mathbf{p},\mathbf{p}'), \qquad (1)$$

where $\omega(\mathbf{p}) = 2E(\mathbf{p}) = 2\sqrt{m^2+\mathbf{p}^2}$, m is the mass of the nucleons and $\mathbf{p}$ is the relative momentum of two nucleons. The connection between the relativistic and non-relativistic NN potentials, *i.e.* V_r and V_{nr}, is defined by the quadratic operator equation [12]

$$V_{nr} = \frac{1}{4m}\left(\omega(\hat{p})V_r + V_r\omega(\hat{p}) + V_r^2\right). \qquad (2)$$

The matrix elements of the relativistic potential can be obtained from the non-relativistic NN potentials by the projection of eq. (2) into the NN basis states $|\mathbf{p}\rangle$

$$\langle \mathbf{p}|V_r|\mathbf{p}'\rangle + \frac{1}{\omega(\mathbf{p})+\omega(\mathbf{p}')}\int d\mathbf{p}''\langle \mathbf{p}|V_r|\mathbf{p}''\rangle\,\langle \mathbf{p}''|V_r|\mathbf{p}'\rangle =$$
$$\frac{4m\langle \mathbf{p}|V_{nr}|\mathbf{p}'\rangle}{\omega(\mathbf{p})+\omega(\mathbf{p}')}. \qquad (3)$$

Table 1. Parameters of the Malfliet-Tjon I potential.

V_A (MeV fm)	μ_A (fm^{-1})	V_R (MeV fm)	μ_R (fm^{-1})
−626.8932	1.550	1438.7228	3.11

In our study we have followed Kamada and Glöckle's strategy [12] to obtain the matrix elements of the relativistic NN potential, *i.e.* $\langle \mathbf{p}|V_r|\mathbf{p}'\rangle$, directly from the non-relativistic one, *i.e.* $\langle \mathbf{p}|V_{nr}|\mathbf{p}'\rangle$ without using PW decomposition. Here we discuss the numerical solution of eq. (3) as a function of the magnitude of the momentum vectors and the angle between them. In our calculations we have used the spin-independent Malfliet-Tjon (MT) potential, which is a superposition of short-range repulsive and long-range attractive Yukawa interactions [44]

$$V_{nr}(\mathbf{p},\mathbf{p}') = \frac{1}{2\pi^2}\left(\frac{V_R}{\mathbf{q}^2+\mu_R^2} + \frac{V_A}{\mathbf{q}^2+\mu_A^2}\right), \qquad (4)$$

where $\mathbf{q} = \mathbf{p}'-\mathbf{p}$. The parameters of the MT-I potential are given in table 1. In order to obtain the matrix elements of the relativistic potential, we have solved eq. (3) by the iteration method. A coordinate system is defined by choosing the relative momentum vector $\mathbf{p}$ parallel to the z-axis and vector $\mathbf{p}'$ in the x-z plane, so that eq. (3) can be written explicitly as

$$V_r(p,p',x') + \frac{1}{\omega(p)+\omega(p')}\int_0^\infty dp''p''^2 \int_{-1}^1 dx'' \int_0^{2\pi} d\phi''$$

$$\times V_r(p,p'',x'')V_r(p'',p',y) = \frac{4mV_{nr}(p,p',x')}{\omega(p)+\omega(p')}, \qquad (5)$$

where

$$x' = \hat{\mathbf{p}}'\cdot\hat{\mathbf{p}},$$
$$x'' = \hat{\mathbf{p}}''\cdot\hat{\mathbf{p}},$$
$$y = \hat{\mathbf{p}}''\cdot\hat{\mathbf{p}}' = x'x'' + \sqrt{1-x'^2}\sqrt{1-x''^2}\cos\phi''. \qquad (6)$$

We start the iteration with

$$V_r^{(0)}(p,p',x') = \frac{4mV_{nr}(p,p',x')}{\omega(p)+\omega(p')}, \qquad (7)$$

and stop it when the calculated relativistic potential satisfies eq. (5) with a relative error of 10^{-6} at each set point (p,p',x'). To speed up the convergence procedure in solving eq. (5) we can redefine the relativistic potential in each step of the iteration as a linear combination of the calculated relativistic potential in the last two successive iterations as

$$V_r^{(n)}(p,p',x') \longrightarrow \frac{\alpha V_r^{(n)}(p,p',x') + \beta V_r^{(n-1)}(p,p',x')}{\alpha+\beta};$$
$$n = 1,2,\ldots. \qquad (8)$$

Kamada and Glöckle have used $\alpha = \beta = 1$ in their calculations for the AV18 potential. Our numerical analysis
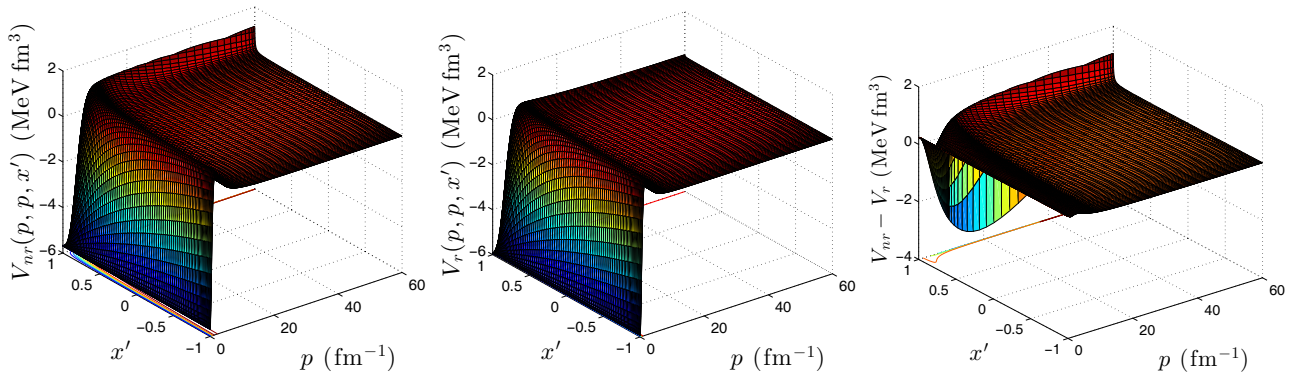
Fig. 1. The matrix elements of the non-relativistic (left panel), the relativistic (middle panel) NN potentials and their differences (right panel) calculated by the MT-I potential as a function of 2B relative momenta $p = p'$ and the angle between them x'.

Table 2. The number of iterations N_{iter}, to reach the convergence in the solution of eq. (5) for MT-I potential as a function of the averaging parameters α and β.

α	β	N_{iter}
1	0	17
1	1	18
2	1	12
3	1	10
4	1	8
5	1	10

shows that the larger values of α can lead to faster convergence in the solution of eq. (5). In table 2 we have shown the number of iterations to reach convergence in eq. (5) for different values of α and β. This indicates that $\alpha = 4$ and $\beta = 1$ leads to faster convergence for the calculation of the relativistic potential from the MT-I bare potential.

For the discretization of the continuous momentum and angle variables we used the Gauss-Legendre quadrature. For the momentum variables a hyperbolic plus linear mapping is used to cover the integration domain $[0, \infty)$ by the subintervals $[0, p_1] \bigcup [p_1, p_2] \bigcup [p_2, p_{max}]$

$$p = \frac{1 + x}{\frac{1}{p_1} + \left(\frac{2}{p_2} - \frac{1}{p_1}\right) x}, \qquad (9)$$

$$p = \frac{p_{max} - p_2}{2} x + \frac{p_{max} + p_2}{2}. \qquad (10)$$

The typical values for p_1, p_2 and p_{max} are 4, 9 and 60 fm^{-1}, respectively. In our calculations we have used 100 mesh points for the momentum variables, 50 mesh points for the spherical and 10 mesh points for the azimuthal angle variables. In each iteration we needed to interpolate on the angle variable y and to avoid extrapolation we have added the extra points ± 1 to the angle mesh points x'. In order to save run time and memory in the solution of eq. (5) we have used the symmetry property of the kernel to calculate the integration over the azimuthal angle ϕ'' on the $[0, \pi/2]$ domain

$$\int_0^{2\pi} \mathrm{d}\phi'' f(\cos\phi'') = 2 \int_0^{\frac{\pi}{2}} \mathrm{d}\phi'' \left[f(\cos\phi'') + f(-\cos\phi'') \right]. \qquad (11)$$

Table 3. The convergence of the matrix elements of the relativistic potential $V_r(p, p', x')$ (in units of MeV fm^3) as a function of the iteration number calculated by the MT-I bare potential in the fixed points ($p = 0.87$ fm^{-1}, $p' = 2.09$ fm^{-1}, $x' = 0, \pm 1$). The values of the MT-I bare potential $V_{nr}(p, p', x')$ are also given.

	$x' = -1$	$x' = 0$	$x' = +1$
	$V_{nr}(p, p', x')$		
	1.1099096	0.7084511	-1.6327025
Iteration #	$V_r(p, p', x')$		
0	1.0525724	0.6718530	-1.5483583
1	0.7838006	0.3920976	-1.8512322
2	0.8895160	0.4979858	-1.7453002
3	0.8853336	0.4938142	-1.7495059
4	0.8848131	0.4932883	-1.7500527
5	0.8847858	0.4932573	-1.7500929
6	0.8847910	0.4932608	-1.7500930
7	0.8847932	0.4932623	-1.7500928
8	0.8847938	0.4932626	-1.7500930
9	0.8847939	0.4932626	-1.7500931
10	0.8847939	0.4932626	-1.7500932
11	0.8847939	0.4932626	-1.7500933
12	0.8847939	0.4932626	-1.7500933

In figs. 1 and 2 we have shown our numerical results for the relativistic potential calculated from the MT-I potential. The bare MT-I potential as well as the difference between the bare and constructed relativistic potentials is also shown. The plots of fig. 1 show the non-relativistic and relativistic potentials as well as their difference as a function of the relative momenta $p = p'$ and the angle between them x'. It seems that the solution of the quadratic equation for the relativistic potential completely changes the structure of the potential at forward angles for diagonal matrix elements $p = p'$, and the relativistic potential is almost smooth in comparison with the non-relativistic potential. The corresponding plots in fig. 2, show the partial wave projection of the non-relativistic and the relativistic potentials and also their differences, calculated from the 3D representation
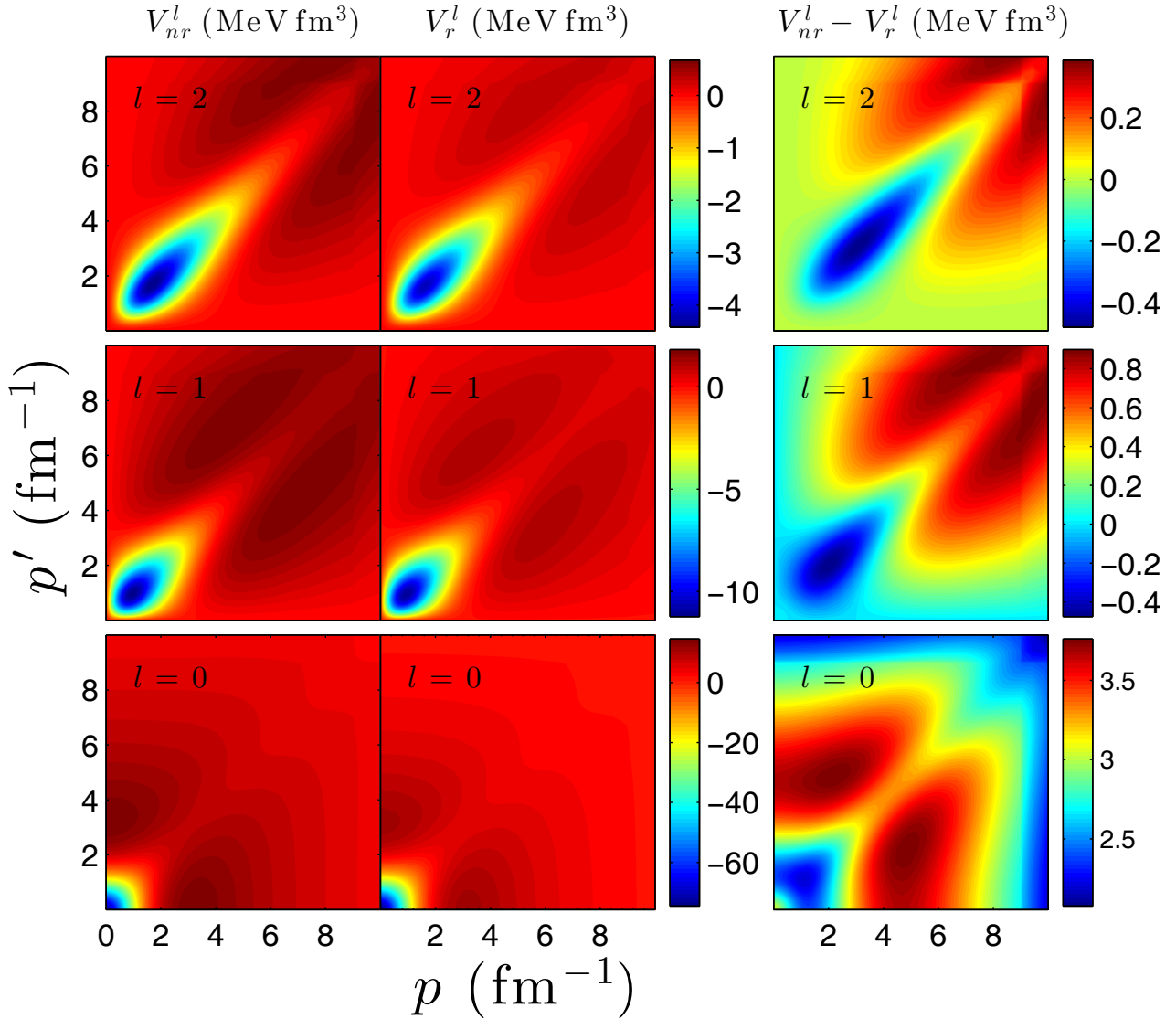
Fig. 2. The matrix elements of the partial wave projection of the non-relativistic (first column), the relativistic (second column) NN potentials and their differences (third column) calculated by the MT-I potential as a function of 2B relative momenta p and p'.

by $V_l(p, p') = 2\pi \int_{-1}^{+1} dx' \, P_l(x') \, V(p, p', x')$, as a function of the relative momenta p and p'. As we can see the matrix elements of the relativistic and non-relativistic potentials are larger for the lower partial waves and consequently their differences become higher.

Table 3 shows an example of the convergence of the matrix elements of the relativistic potential by iteration number for the fixed points ($p = 0.87\,\text{fm}^{-1}$, $p' = 2.09\,\text{fm}^{-1}$, $x' = 0, \pm 1$) for $\alpha = 2$ and $\beta = 1$.

3 Numerical tests of the relativistic potential

3.1 NN bound state

The total Hamiltonian of two interacting nucleons in the center-of-mass system is

$$\langle \mathbf{p} | H | \mathbf{p'} \rangle = H_0(\mathbf{p}) \, \delta(\mathbf{p} - \mathbf{p'}) + V_{nr}(\mathbf{p}, \mathbf{p'}), \qquad (12)$$

where $H_0(\mathbf{p}) = \frac{\mathbf{p}^2}{m}$ is the free Hamiltonian, $V_{nr}(\mathbf{p}, \mathbf{p'})$ is the non-relativistic NN interaction and $\mathbf{p}(\mathbf{p'})$ is the initial (final) relative momentum of two nucleons. The Lippmann-Schwinger equation for the two-nucleon bound state is given as

$$|\psi_d\rangle = \frac{1}{E_d - H_0} V_{nr} |\psi_d\rangle, \qquad (13)$$

which can be represented in momentum space as the following eigenvalue equation:

$$\psi_d(\mathbf{p}) = \frac{1}{E_d - \frac{\mathbf{p}^2}{m}} \int d\mathbf{p'} \, V_{nr}(\mathbf{p}, \mathbf{p'}) \, \psi_d(\mathbf{p'}). \qquad (14)$$

The relativistic Schrödinger equation for the two-nucleon bound state has the form

$$h|\psi_d\rangle = M_d |\psi_d\rangle, \qquad (15)$$

Table 4. Deuteron binding energy calculated for MT-I bare and relativistic potentials and their relative difference.

E_d^{nr} (MeV)	E_d^r (MeV)	$(E_d^{nr} - E_d^r)/E_d^{nr}$ %
-2.23100	-2.23229	0.05782
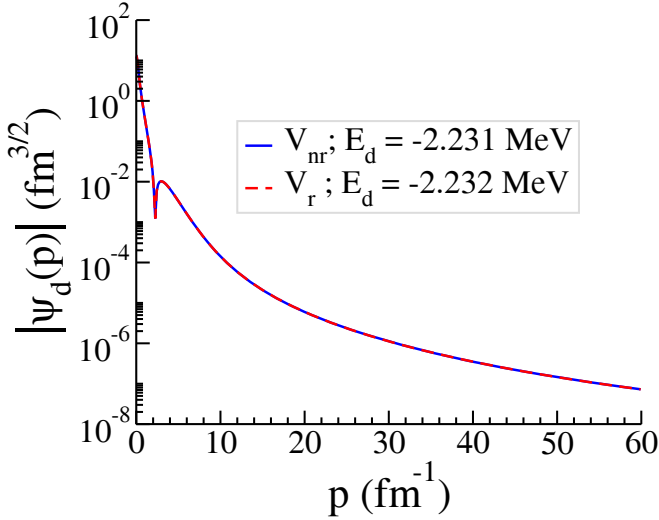
Fig. 3. The deuteron wave function calculated by the MT-I bare and relativistic potentials.

where M_d is the deuteron mass. The relativistic deuteron wave function $|\psi_d\rangle$ satisfies the eigenvalue equation

$$\psi_d(\mathbf{p}) = \frac{1}{M_d - \omega(\mathbf{p})} \int d\mathbf{p}' \, V_r(\mathbf{p}, \mathbf{p}') \, \psi_d(\mathbf{p}'). \quad (16)$$

Our numerical results for the deuteron binding energy and wave function calculated by relativistic and non-relativistic potentials are given in table 4 and fig. 3. As we can see the constructed relativistic potential preserves the deuteron binding energy obtained by the bare MT-I potential with high accuracy and the relative percentage difference of about 0.06.

3.2 NN scattering

The inhomogeneous Lippmann-Schwinger equation which describes the two-nucleon scattering can be represented in momentum space as

$$T_{nr}(\mathbf{p}, \mathbf{p}'; E) = V_{nr}(\mathbf{p}, \mathbf{p}') + \int d\mathbf{p}'' \frac{V_{nr}(\mathbf{p}, \mathbf{p}'')}{\frac{p_0^2}{m} - \frac{\mathbf{p}''^2}{m} + i\epsilon} T_{nr}(\mathbf{p}'', \mathbf{p}'; E). \quad (17)$$

The differential cross section for elastic NN scattering as a function of the incident projectile energy $E_{lab} = 2E_{cm} = \frac{2p_0^2}{m}$ is given by

$$\frac{d\sigma}{d\Omega} = (2\pi)^4 \left(\frac{m}{2}\right)^2 |T_{sym}(p_0, p_0, x')|^2, \quad (18)$$

Table 5. The total elastic NN scattering cross section as a function of the on-shell momentum p_0 calculated by the MT-I bare and relativistic potentials.

p_0 (MeV)	σ_{nr} (mb)	σ_r (mb)	$|(\sigma_{nr} - \sigma_r)/\sigma_{nr}|$%
1	15274.4	15273.3	0.00720
10	14526.4	14525.5	0.00620
25	11485.5	11484.9	0.00522
50	6367.46	6367.31	0.00236
75	3432.10	3432.08	0.00058
100	1926.16	1926.17	0.00052
200	297.580	297.586	0.00202
300	129.008	129.015	0.00543
400	94.6592	94.6631	0.00412
500	72.6167	72.6201	0.00468
600	56.9070	56.9111	0.00720

where

$$T_{sym}(p_0, p_0, x') = T_{nr}(p_0, p_0, x') + T_{nr}(p_0, p_0, -x'). \quad (19)$$

Consequently, the total cross section can be obtained directly from the differential cross section as

$$\sigma = (2\pi)^5 \left(\frac{m}{2}\right)^2 \int_{-1}^{+1} dx' \, |T_{sym}(p_0, p_0, x')|^2. \quad (20)$$

The relativistic NN scattering can be described by the relativistic form of the Lippmann-Schwinger equation as

$$T_r(\mathbf{p}, \mathbf{p}') = V_r(\mathbf{p}, \mathbf{p}') + \int d\mathbf{p}'' \frac{V_r(\mathbf{p}, \mathbf{p}'')}{\omega(p_0) - \omega(p'') + i\epsilon} T_r(\mathbf{p}'', \mathbf{p}'). \quad (21)$$

The relativistic differential and total cross sections can be obtained by eqs. (18) and (20) and by replacing m with $\sqrt{m^2 + p_0^2}$.

In table 5, our numerical results for the total elastic NN scattering cross sections obtained by the constructed relativistic potential from the MT-I potential are given as a function of the on-shell momentum p_0. As we can see the relativistic total cross sections are in excellent agreement with the corresponding non-relativistic cross sections and have a percentage relative difference of less than 0.007. NN phase shifts in the PW scheme are calculated by

$$\delta_l(p_0) = \arctan\left(\frac{\text{Im}\, T_l(p_0)}{\text{Re}\, T_l(p_0)}\right), \quad (22)$$

where the partial wave T-matrix, i.e. $T_l(p_0)$, can be obtained from the 3D form of the T-matrix, i.e. $T(p_0, p_0, x')$, as

$$T_l(p_0) = 2\pi \int_{-1}^{+1} dx' \, P_l(x') \, T(p_0, p_0, x'). \quad (23)$$

In table 6, we have shown our numerical results for the s- and p-wave NN phase shifts as a function of the on-shell momentum p_0 calculated from the projection of the

Table 6. The s- and p-wave phase shifts, δ_0 and δ_1, calculated by the MT-I bare and relativistic potentials as a function of the on-shell momentum p_0.

p_0 (MeV)	δ_0^{nr}	δ_0^r	$|(\delta_0^{nr} - \delta_0^r)/\delta_0^{nr}|\%$
1	178.399202	178.399259	0.00003
10	164.191097	164.191642	0.00033
25	142.727577	142.728682	0.00077
50	115.599510	115.600883	0.00119
75	96.723079	96.724553	0.00152
100	82.604149	82.605322	0.00142
200	46.516325	46.517103	0.00167
300	24.195385	24.196576	0.00492
400	8.220831	8.220032	0.00972
500	176.141274	176.139179	0.00119
600	166.764703	166.759452	0.00315

p_0 (MeV)	δ_1^{nr}	δ_1^r	$|(\delta_1^{nr} - \delta_1^r)/\delta_1^{nr}|\%$
1	0.000015228	0.000015228	0.0017533
10	0.01520323	0.015203706	0.0030894
25	0.235486179	0.235489846	0.0015574
50	1.820265835	1.820327160	0.0033690
75	5.735591957	5.735736050	0.0025123
100	12.07379026	12.07410200	0.0025819
200	35.51818548	35.51899747	0.0022861
300	36.92310114	36.92426648	0.0031561
400	31.28393516	31.28424025	0.0009752
500	24.51728521	24.51716984	0.0004706
600	18.01488447	18.01311044	0.0098475

3D form of the non-relativistic and relativistic T-matrices by eq. (23). As we can see the relativistic s- and p-wave NN phase shifts are in excellent agreement with the corresponding non-relativistic ones and have a relative percentage difference of less than 0.004 and 0.01, respectively.

4 Discussion and outlook

In this paper, we have used a three-dimensional approach to formulating the relativistic nucleon-nucleon potential as a function of the two-body relative momentum vectors. The quadratic equation which connects the relativistic and non-relativistic nucleon-nucleon interactions is presented in momentum space as a three-dimensional integral equation. For the first numerical implementation, the integral equation is solved by the spin-independent Malfliet-Tjon potential, and the matrix elements of the relativistic potential are calculated as a function of the two-body relative momenta and the angle between them. Our numerical analysis confirms that the two-body observables calculated from the relativistic potential are preserved. The extension of this formalism to realistic nucleon-nucleon interactions with spin degrees of freedom in a momentum-helicity basis state is currently underway.

References

1. H. Wita?a, J. Golak, R. Skibi?ski, W. Glöckle, H. Kamada, W.N. Polyzou, Phys. Rev. C **83**, 044001 (2011) **88**, 069904(E) (2013).
2. H. Wita?a, J. Golak, R. Skibi?ski, W. Glöckle, W.N. Polyzou, H. Kamada, Phys. Rev. C **77**, 034004 (2008).
3. K. Sekiguchi *et al.*, Phys. Rev. Lett. **95**, 162301 (2005).
4. H. Wita?a, J. Golak, W. Glöckle, H. Kamada, Phys. Rev. C **71**, 054001 (2005).
5. H. Wita?a, J. Golak, R. Skibi?ski, W. Glöckle, W. Polyzou, H. Kamada, Few-Body Syst. **49**, 61 (2011).
6. T. Lin, Ch. Elster, W.N. Polyzou, W. Glöckle, Phys. Lett. B **660**, 345 (2008).
7. T. Lin, Ch. Elster, W.N. Polyzou, W. Glöckle, Phys. Rev. C **76**, 014010 (2007).
8. H. Wita?a, J. Golak, R. Skibnski, W. Glöckle, W.N. Polyzou, H. Kamada, Mod. Phys. Lett. A **24**, 871 (2009).
9. H. Kamada, W. Glöckle, H. Wita?a, J. Golak, R. Skibi?ski, W.N. Polyzou, Ch. Elster, Mod. Phys. Lett. A **24**, 809 (2009).
10. H. Kamada, W. Glöckle, J. Golak, Ch. Elster, Phys. Rev. C **66**, 044010 (2002).
11. W. Glöckle, T.S.H. Lee, F. Coester, Phys. Rev. C **33**, 709 (1986).
12. H. Kamada, W. Glöckle, Phys. Lett. B **655**, 119 (2007).
13. H. Kamada, W. Glöckle, Phys. Rev. Lett. **80**, 2547 (1998).
14. M.R. Hadizadeh, Ch. Elster, W.N. Polyzou, EPJ Web of Conferences **113**, 03011 (2016).
15. M.R. Hadizadeh, K.A. Wendt, Ch. Elster, EPJ Web of Conferences **113**, 08008 (2016).
16. M.R. Hadizadeh, Ch. Elster, W.N. Polyzou, Phys. Rev. C **90**, 054002 (2014).
17. M.R. Hadizadeh, Prog. Theor. Exp. Phys. **2014**, 043D01 (2014).
18. M.R. Hadizadeh, L. Tomio, S. Bayegan, Phys. Rev. C **83**, 054004 (2011).
19. J. Golak, W. Glöckle, R. Skibi?ski, H. Wita?a, D. Rozpedzik, K. Topolnicki, I. Fachruddin, Ch. Elster, A. Nogga, Phys. Rev. C **81**, 034006 (2010).
20. W. Glöckle, I. Fachruddin, Ch. Elster, J. Golak, R. Skibi?ski, H. Wita?a, Eur. Phys. J. A **43**, 339 (2010).
21. W. Glöckle, Ch. Elster, J. Golak, R. Skibi?ski, H. Wita?a, H. Kamada, Few-Body Syst. **47**, 25 (2010).
22. S. Bayegan, M.A. Shalchi, M.R. Hadizadeh, Phys. Rev. C **79**, 057001 (2009).
23. T. Lin, Ch. Elster, W.N. Polyzou, H. Wita?a, W. Glöckle, Phys. Rev. C **78**, 024002 (2008).
24. T. Lin, Ch. Elster, W.N. Polyzou, W. Glöckle, Phys. Lett. B **660**, 345 (2008).
25. S. Bayegan, M.R. Hadizadeh, W. Glöckle, Prog. Theor. Phys. **120**, 887 (2008).

26. Bayegan, M. Harzchi, M.R. Hadizadeh, Nucl. Phys. A **814**, 21 (2008).
27. S. Bayegan, M. Harzchi, M.A. Shalchi, Nucl. Phys. A **832**, 1 (2010).
28. M. Harzchi, S. Bayegan, Eur. Phys. J. A **46**, 271 (2010).
29. M. Radin, H. Ghasemi, Nucl. Phys. A **945**, 269 (2016).
30. S. Bayegan, M.R. Hadizadeh, M. Harzchi, Phys. Rev. C **77**, 064005 (2008).
31. M. Radin, Sh. Babaghodrat, M. Monemzadeh, Phys. Rev. D **90**, 047701 (2014).
32. M.R. Hadizadeh, S. Bayegan, Eur. Phys. J. A **36**, 201 (2008).
33. M.R. Hadizadeh, S. Bayegan, Few-Body Syst. **40**, 171 (2007).
34. H. Liu, Ch. Elster, W. Glöckle, Phys. Rev. C **72**, 054003 (2005).
35. I. Fachruddin, W. Glöckle, Ch. Elster, A. Nogga, Phys. Rev. C **69**, 064002 (2004).
36. I. Fachuddin, Ch. Elster, W. Glöckle, Phys. Rev. C **68**, 054003 (2003).
37. H. Liu, Ch. Elster, W. Glöckle, Few-Body Syst. **33**, 241 (2003).
38. I. Fachruddin, Ch. Elster, W. Glöckle, Phys. Rev. C **62**, 044002 (2000).
39. I. Fachruddin, Ch. Elster, W. Glöckle, Phys. Rev. C **63**, 054003 (2001).
40. F. Coester, Steven C. Pieper, F.J.D. Serduke, Phys. Rev. C **11**, 1 (1975).
41. B.D. Keister, W.N. Polyzou, Phys. Rev. C **73**, 014005 (2006).
42. B. Bakamjian, L.H. Thomas, Phys. Rev. **92**, 1300 (1953).
43. R. Fong, J. Sucher, J. Math. Phys. **5**, 956 (1964).
44. R.A. Malfliet, J.A. Tjon, Nucl. Phys. A **127**, 161 (1969).